THE JOURNAL OF PHYSICAL CHEMISTRY C

Article

pubs.acs.org/JPCC

Two-Step Decomposition of Plasmon Coupling in Plasmonic Oligomers

Meng Wang,[†] Min Cao,[†] Zhirui Guo,[‡] and Ning Gu*,[†]

[†]State Key Laboratory of Bioelectronics and Jiangsu Key Laboratory for Biomaterials and Devices, School of Biological Science and Medical Engineering, Southeast University, Nanjing 210096, People's Republic of China

[‡]The Second Affiliated Hospital of Nanjing Medical University, Nanjing 210011, People's Republic of China

Supporting Information

ABSTRACT: Plasmon coupling in plasmonic oligomers gives rise to many unique optical properties including electromagnetically induced transparency and Fano resonances. Controlling over the optical properties of plasmonic oligomers requires a deep understanding of the physical mechanisms. Herein, we first examine the near and far field optical properties of silver pentamer by the coupled dipole approximation. It is shown that the Fano-like resonance in the pentamer is analogous to the spectrum of a heterogeneous plasmonic dimer. Therefore, we propose a subgroup decomposition method for predicting the spectrum profiles of the oligomers. In the decomposition procedure, the oligomer is divided into simple subgroups in terms of the arrangement of nanoparticles and incident polarization, and the optical response of the oligomer is determined by the coupling of the subgroups. We further investigate its validity in strongly coupled plasmonic oligomers through the generalized multiparticle Mie solution. The optical properties of the close-packed oligomers can also be easily modulated by means of the decomposition method, which provides a flexible tool for the optimal design of plasmonic nanostructures.

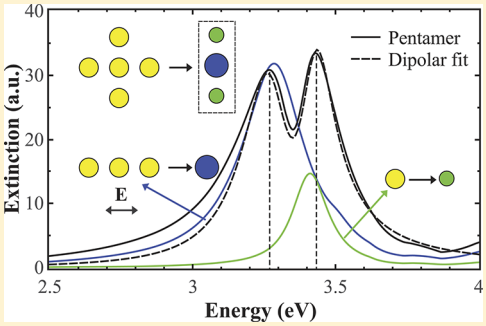

INTRODUCTION

The optical properties of metal nanoparticles are dominated by coherent oscillations of conduction band electrons, known as localized surface plasmon resonance (LSPR).[1−3] Oligomers of plasmonic nanoparticles, consisting of metal nanoparticles that interact via their near fields, have recently attracted much attention due to their unique optical properties as well as their remarkable potential in LSPR sensing.[4] Moreover, the spectrum profiles of plasmonic oligomers can be tuned directly by changing the geometry and composition of individual nanoparticle, facilitating the study of the nature of electromagnetic coupling.[5−8]

Because surface plasmons are well described as classical oscillators, plasmonic oligomers are in essence systems of coupled oscillators, supporting a wide range of phenomena based on coupled oscillator physics including electromagnetically induced transparency (EIT)[9,10] and Fano resonance.[11−13] Fano resonance originates from the spectral overlap of broad superradiant (bright) and sharp subradiant (dark) resonance modes.[14] It can be induced by symmetry breaking due to the mixing of the bright dipole plasmon mode with dark multipolar plasmon modes.[15,16] Because plasmonic coupling depends on the relative phase of the constituent oscillators, Fano resonances are highly sensitive to variations in geometry and dielectric environment.[17] Recently, plasmonic oligomers are also found to exhibit Fano resonances. Unlike most of the other plasmonic nanostructures, Fano resonance in oligomers is generated by dipole plasmon modes with different oscillation phases arising from various elements without the need to excite multipolar plasmon modes.[18,19] Such Fano resonances can be viewed as the realization of EIT, which is equivalent to the case of interference between two dressed states with closely spaced resonant frequencies.[17,20]

Controlling over the optical properties of plasmonic oligomers for specific applications requires a deep understanding of the physical mechanisms. Hentschel et al.[4] examined the role of individual nanoparticles for the collective behavior in plasmonic oligomers. Very recently, Rahmani et al.[21] proposed a recipe to tailor the spectral profile in plasmonic oligomers. They demonstrated that the extinction spectra of oligomers could be decoded into two individual contributions from their subgroups. In this study, we show that the Fano-like resonance in plasmonic oligomers is analogous to the EIT phenomenon in detuned plasmonic heterodimers. Based on this observation, we propose a two-step decomposition method for estimating the radiative properties of plasmonic oligomers. We first divide the oligomer into several subgroups, whose axes are parallel to the incident electric polarization. The spectrum of each subgroup is characterized by one-dimensional coupling under longitudinal excitation. Subsequently, we fit the subgroups to dipolar scatters by Drude model, thus, the spectrum of the oligomer is determined by the coupling of the

Received: January 13, 2013
Revised: March 31, 2013
Published: May 13, 2013

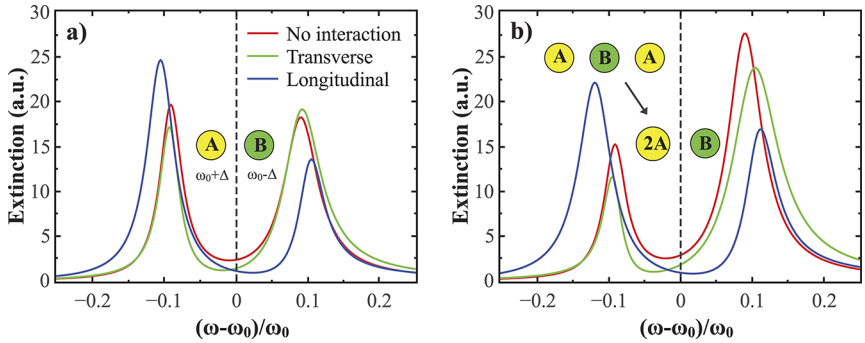

Figure 1. Calculated extinction spectra of a heterogeneous dimer (a) and trimer (b) under transverse and longitudinal excitations by CDA. The colors of the sphere indicate the type of the plasmonic particles.

subgroups. By means of this method, it is flexible to predict and control the resonance profile without the need of further calculation. The validity of this method for strongly coupled plasmonic nanostructures is also investigated by the generalized multiparticle Mie (GMM) solution.

METHODOLOGY

In the coupled dipole approximation (CDA), the particles are described as electric dipoles with electric polarizabilities α_n. Consider an ensemble of spherical particles with radii a_n located at points r_n, the electric dipole moments p_n are induced by the incident field on each particle and the fields scattered by all the other particles, which can be expressed by the coupled dipole equations[22]

$$p_n = \alpha_n[E_n^0 + \sum_{m\neq n}^{N} \hat{G}_{mn}p_m] \tag{1}$$

where E_n^0 is the incident electric field at center of the nth particle, the term $\hat{G}_{mn}p_m$ gives the dipole radiation field created by the dipole p_m at the point r_n, $\hat{G}_{mn}$ is the regular part of the free space dyadic Greens function, and the quasi−static polarizability α_n is given by

$$\alpha_n = a_n^3\frac{\varepsilon_n - 1}{\varepsilon_n + 2} \tag{2}$$

The dielectric responses of particles obey the Drude form

$$\varepsilon_n = 1 - \frac{\omega_{pn}^2}{\omega^2 + i\gamma_n\omega} \tag{3}$$

where ω_{pn} and γ_n are the plasma frequency and damping frequency of nth particle. The polarizabilities of the nanospheres can be written as

$$\alpha_n = a_n^3\frac{\varepsilon_n - 1}{\varepsilon_n + 2} = \frac{a_n^3\omega_{fn}^2}{\omega_{fn}^2 - \omega^2 - i\gamma_n\omega} \tag{4}$$

where $\omega_{fn} = \omega_{pn}/(3)^{1/2}$ is the Fröhlich frequency (LSPR frequency of the nth sphere).

The induced electric dipole moments of each particle can be obtained by solving the system of equations (eq 1), and the total extinction cross section are calculated by

$$C_{ext} = 4\pi k\mathrm{Im}\sum_{n=1}^{N}(p_n\cdot E_n^{0*}) \tag{5}$$

For planar particle aggregates at normal incidence, the incident field E^0 on each particle has the same phase. Thus, the extinction cross section of the aggregate is proportional to the imaginary part of total dipole moment ($p^{Tot} = \Sigma p_n$).

RESULTS AND DISCUSSION

In what follows, we consider two heterogeneous plasmonic particles (a_1,a_2), that is, detuned plasmonic heterodimers. The LSPR frequencies of the plasmonic particles are equally detuned from the central frequency $\omega_{f(1,2)} = \omega_0 \pm \Delta$, where ω_0 and Δ are the center and detuning frequency. The solution to the system of coupled equations eq 1 for heterodimers can be expressed as

$$p_1 = \frac{\alpha_1 + \alpha_1\alpha_2 G}{1 - \alpha_1\alpha_2 G^2}$$
$$p_2 = \frac{\alpha_2 + \alpha_1\alpha_2 G}{1 - \alpha_1\alpha_2 G^2} \tag{6}$$

For dimer axis aligns perpendicular (transverse excitation) and parallel (longitudinal excitation) to the electric polarization axis, the dipole interaction functions $G^{\perp}$ and $G^{\parallel}$ are given by

$$G^{\perp} = k^3e^{ikd}\left(\frac{1}{kd} + \frac{i}{(kd)^2} - \frac{1}{(kd)^3}\right) \tag{7}$$

$$G^{\parallel} = k^3e^{ikd}\left(-\frac{2i}{(kd)^2} + \frac{2}{(kd)^3}\right) \tag{8}$$

where d is the interparticle distance in terms of the center to center spacing of particles. If the interparticle distance is much smaller than the incident wavelength ($kd \to 0$), we have the following limiting relations: $G^{\perp} \to -1/d^3$, $G^{\parallel} \to -2/d^3$. For frequency, $\omega = \omega_0 + \delta$ close to the center frequency ($\delta \ll \omega_0$), the imaginary part of the total dipole moment can be expressed with the first-order approximation as

$$\mathrm{Im}[p^{Tot}] = \frac{\gamma\omega_0[4A(\delta+\Delta)^2 + 4B(\delta-\Delta)^2 - 8ABG\omega_0\delta + (A+B)(\gamma^2 + ABG^2\omega_0^2)]}{16(\delta^2-\Delta^2)^2 + 8\gamma^2(\delta^2+\Delta^2) + ABG^2\omega_0^2(2\gamma^2 - 8\delta^2 + 8\Delta^2 + ABG^2\omega_0^2) + \gamma^4} \tag{9}$$

dx.doi.org/10.1021/jp4004054 | J. Phys. Chem. C 2013, 117, 11713−11717

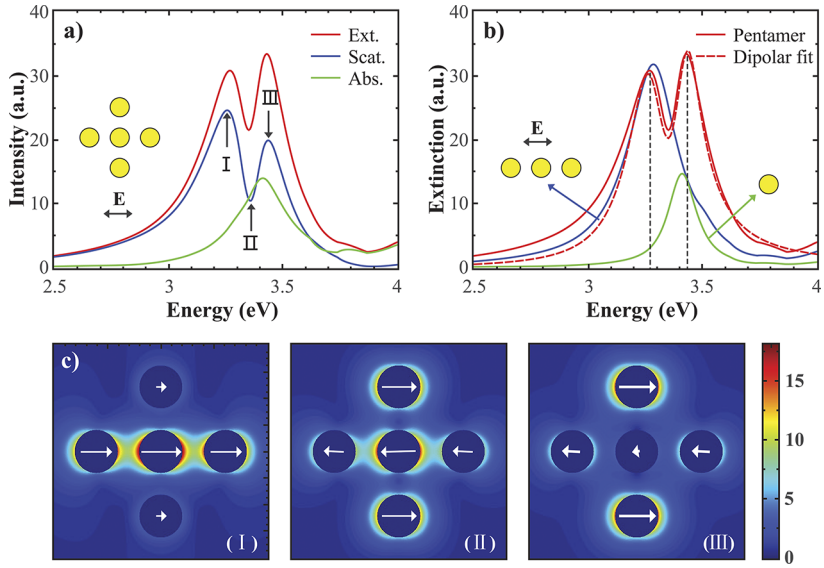

Figure 2. (a) Extinction, scattering and absorption cross sections of a pentamer by dynamic CDA, the pentamer consists five silver nanoparticles (a = 25 nm) with gap size g = 25 nm. (b) Decomposition and dipolar fit of scattering spectrum for the pentamer. (c) Near field distributions at three specific frequencies as marked in (a).

where $A = a_1^3$, $B = a_2^3$ (see detailed derivation in Supporting Information).

Figure 1a shows the extinction spectra of a heterodimer consisting of two plasmonic particles ($a_1 = a_2 = 25$ nm) with interparticle spacing d = 75 nm. The center frequency, detuning frequency and damping frequency are 2.75, 0.25, and 0.05 eV, respectively. In all cases, the extinction spectra have two peaks corresponding to the plasmon frequencies of each sphere, and there is a minimum near the center frequency. The interaction between particles leads to changes in the absolute maximum values and deviations of resonance frequencies.

For transverse excitations, the spectrum changes very little compared with the case of noninteracting dipoles (red line). For longitudinal excitation, the plasmon coupling induces a distinct red shift of the low-energy resonance and a blue shift of the high-energy resonance. The suppression of extinction is observed near the center frequency, which is related to the EIT phenomenon.

The above results can be explained by eq 9 mathematically. The two local maxima of $\mathrm{Im}[p^{\mathrm{Tot}}]$ are at

$$\delta \approx \pm\frac{1}{2}\sqrt{4\Delta^2 - \gamma^2 + ABG^2\omega_0^2}$$

corresponding to the coupled plasmon peak frequency. The interaction function G determines the plasmon resonance shifts. $\mathrm{Im}[p^{\mathrm{Tot}}]$ has a local minimum point at

$$\delta \approx \frac{-A\Delta + B\Delta + ABG\omega_0}{A + B}$$

which indicates the extinction minimum frequency deviation to the center frequency. The minimum frequency deviations for transverse and longitudinal excitations are in opposite directions due to the opposite signs of $G^{\perp}$ and $G^{\parallel}$.

For a detuned plasmonic heterotrimer, the extinction profile is similar to that of the heterodimer (see Figure 1b). In fact, if we ignore the coupling between the side particles, the extinction of the heterotrimer can be determined by enlarging the radius of particle A ($a' = 3(2a)^{1/2}$, see more details in Supporting Information).

We now analyze the optical properties of a plasmonic pentamer which consists of five silver nanoparticles (a = 25 nm) with gap size g = 25 nm. For these silver nanoparticles, the quasistatic polarizability is not adjusted due to the retardation effect (Figure S1), we characterize each nanoparticle by the dynamic dipole polarizability which is the first order electric term of the Mie coefficients.[23] Figure 2a shows the optical properties of the pentamer calculated by the dynamic CDA method. The dielectric functions for silver are taken from the data of Johnson and Christy.[24] The extinction and scattering spectra are characterized by two peaks separated by a remarkable dip. Such a dip occurs due to the dipole moments with different oscillation phases arising from various nanoparticles. The near field distributions at three specific frequencies are plotted in Figure 2c, in which the white arrows represent the dipole moment of the particle. At the low-energy resonance frequency (I), all the nanoparticles are oscillating in the same phase, indicating a superradiant plasmon mode. Only the horizontal middle three particles of the pentamer are excited, while the vertical outer two particles have very weak dipole moments. At the dip resonance frequency (II), the middle three particles and vertical outer two particles are both excited featuring oppositely induced electric dipoles. The total dipole moment is greatly reduced resulting in suppression of scattering. At the high-energy resonance frequency (III), the orientations of the dipole moments are similar to the case of dip frequency. However, the dipole moment of the central particle is very weak.

To explore the subgroup contribution to the pentamer extinction, the extinctions of the middle trimer and outer particles are plotted in Figure 2b, respectively. The LSPR frequencies of the trimer and the individual particles are 3.28 and 3.41 eV, which are very close to the two spectral peaks of the pentamer extinction. The deviation of the subgroup LSPR frequencies from pentamer is analogous to the case of detuned plasmonic heterodimers, which means that the extinction of the pentamer can be approximated as the result of the coupling between the trimer and vertical outer particles. Therefore, we fit the trimer and single particle to dipolar scatters by Drude

dx.doi.org/10.1021/jp4004054 | J. Phys. Chem. C 2013, 117, 11713−11717

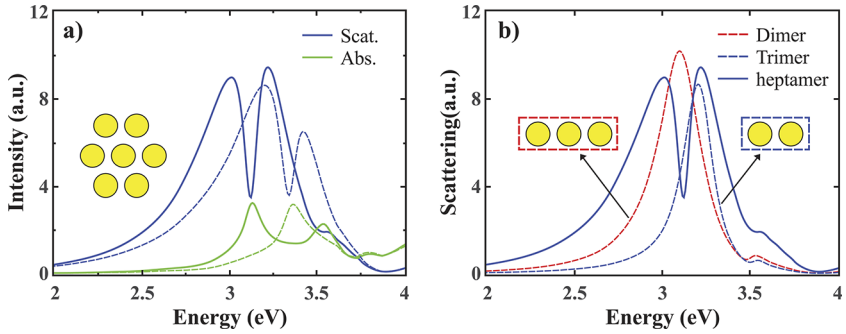

Figure 3. (a) Scattering and absorption cross sections of a heptamer consisting of seven silver nanoparticles (a = 25 nm) with gap size d = 10 nm, the solid and dashed lines correspond to the results of dynamic CDA and GMM theory, respectively. (b) Decomposition of scattering spectrum for the heptamer.

model in terms of the spectral feature, and then calculate the optical properties of the coupling dipolar scatters instead of the pentamer (see more details in Supporting Information). The dash line in Figure 2b shows the extinction spectrum of the coupling dipolar scatters calculated by CDA method, which is in good agreement with that of the pentamer.

Thus, we propose a two-step decomposition method for estimating the radiative properties of plasmonic oligomers. The first step is to divide the oligomer into subgroups in terms of the incident electric polarization. The axis of each group is parallel to the incident electric polarization. The spectrum of each subgroup is characterized by one-dimensional coupling under longitudinal excitation. Second, we fit the subgroups to dipolar scatters in terms of the spectral features, and the optical properties of the oligomers can be determined by the coupling of the subgroups.

Our decomposition is different from the earlier work by Rahmani et al.[21] The coupling between subgroups is unnegligible in our method. It should be pointed out the coupling of subgroups is under a mixture of transverse and longitudinal excitations (Figure S2). However, the coupling strength is relatively weak, which means the longitudinal mode of the subgroup dominates the optical response of the oligomer.

Next, we examine the validity of the decomposition in strongly coupled plasmonic oligomers by GMM method, which is an analytical solution of scattering by an ensemble of nonoverlapping spheres with arbitrary position and size.[25,26] Figure 3a shows the calculated spectra of a silver heptamer with gap size of 10 nm, the dashed line corresponds to the results of the dynamic CDA method. There is a significant difference between the results of the two methods due to the absence of higher order multipoles within CDA. For a single silver nanoparticle (a = 25 nm), multipoles are negligible with respect to dipolar one. In close-packed oligomers, multipolar plasmon modes can be excited by strong near-field coupling, resulting in the red shifts of the resonances. Both absorption spectra show a peak at the corresponding scattering dip, which appears for a plasmonic Fano resonance in large nanoclusters. However, the decomposition method still works well, as shown in Figure 3b. The shifts of the resonance frequencies are more remarkable due to the strong coupling between the subgroups.

Finally, we show the flexibility of the decomposition method for controlling the plasmon coupling (see Figure 4). We change the gap size of the middle trimer g_t to 5 nm. The decreasing separation results in a red shift of the dipolar plasmon resonances of the timer. As a result, the low-energy resonance

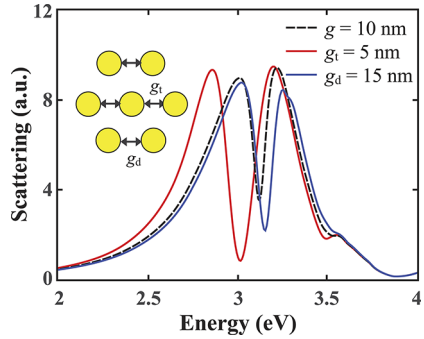

Figure 4. Tuning of plasmon resonance of silver heptamer. The dashed line corresponds to the scattering cross section of the heptamer with gap size of 10 nm.

and Fano dip frequencies of the heptamer have a red shift (red line). However, the high-energy resonance changes very little. In the same manner, we can change the high-energy resonance by changing the gap size of the dimer g_d of the dimers (blue line).

CONCLUSION

In summary, we propose a decomposition method for estimating the radiative properties of plasmonic oligomers. We demonstrate that the Fano-like resonance in plasmonic oligomers results from the interaction between detuned dipolar scatters with different resonant frequencies. We show that spectrum profiles of the oligomers are determined by the coupling of the subgroups in terms of the arrangement of nanoparticles and incident polarization. In this manner, one can easily control the behaviors of the plasmonic coupling in oligomers. Although this method is developed within the CDA approach ignoring the higher order multipoles, the further calculations by GMM theory indicate that it is also applicable for strongly coupled plasmon oligomers. We expect that this study can help to understand the optical properties of the complex plasmonic nanostructures, and provide a flexible method for the optimal design of plasmonic nanostructures for specific applications.

ASSOCIATED CONTENT

Supporting Information

Derivation of the total dipole moments of detuned plasmonic heterodimers, derivation of the effective radius for the plasmonic trimer, comparison of the optical cross sections calculated by CDA and GMM for silver pentamer, decom-

dx.doi.org/10.1021/jp4004054 | J. Phys. Chem. C 2013, 117, 11713−11717

position details, and parameters for the silver pentamer. This material is available free of charge via the Internet at http://pubs.acs.org.

AUTHOR INFORMATION

Corresponding Author

*Tel.: +86(0)25-83272476. Fax: +86(0)25-83272460. E-mail: guning@seu.edu.cn.

Notes

The authors declare no competing financial interest.

ACKNOWLEDGMENTS

We acknowledge the support to this research from the National Important Basic Research Program of China (2011CB933503), the Special Development of Project on National Key Scientific Instruments and Equipment of China (2011YQ03013403), the National Natural Science Foundation of China (61127002), and the Basic Research Program of Jiangsu Province (BK2009013).

REFERENCES

(1) Maier, S. A., Ed. *Plasmonics: Fundamentals and Applications*; Springer: New York, 2006.
(2) Kreibig, U., Vollmer, M., Eds. *Optical Properties of Metal Clusters*; Springer: New York, 1995.
(3) Kelly, K. L.; Coronado, E.; Zhao, L. L.; Schatz, G. C. The Optical Properties of Metal Nanoparticles: The Influence of Size, Shape, and Dielectric Environment. *J. Phys. Chem. B* **2003**, *107*, 668−677.
(4) Hentschel, M.; Dregely, D.; Vogelgesang, R.; Giessen, H.; Liu, N. Plasmonic Oligomers: The Role of Individual Particles in Collective Behavior. *ACS Nano* **2011**, *5*, 2042−2050.
(5) Halas, N. J.; Lal, S.; Chang, W.-S.; Link, S.; Nordlander, P. Plasmons in Strongly Coupled Metallic Nanostructures. *Chem. Rev.* **2011**, *111*, 3913−3961.
(6) Ye, J.; Wen, F.; Sobhani, H.; Lassiter, J. B.; Dorpe, P. V.; Nordlander, P.; Halas, N. J. Plasmonic Nanoclusters: Near Field Properties of the Fano Resonance Interrogated with SERS. *Nano Lett.* **2012**, *12*, 1660−1667.
(7) Lassiter, J. B.; Sobhani, H.; Knight, M. W.; Mielczarek, W. S.; Nordlander, P.; Halas, N. J. Designing and Deconstructing the Fano Lineshape in Plasmonic Nanoclusters. *Nano Lett.* **2012**, *12*, 1058−1062.
(8) Sheikholeslami, S. N.; Garcia-Etxarri, A.; Dionne, J. A. Controlling the Interplay of Electric and Magnetic Modes via Fano-Like Plasmon Resonances. *Nano Lett.* **2011**, *11*, 3927−3934.
(9) Harris, S. E. Electromagnetically Induced Transparency. *Phys. Today* **1997**, *50*, 36−42.
(10) Fleischhauer, M.; Imamoglu, A.; Marangos, J. P. Electromagnetically Induced Transparency: Optics in Coherent Media. *Rev. Mod. Phys.* **2005**, *77*, 633−673.
(11) Francescato, Y.; Giannini, V.; Maier, S. A. Plasmonic Systems Unveiled by Fano Resonances. *ACS Nano* **2012**, *6*, 1830−1838.
(12) Miroshnichenko, A. E.; Flach, S.; Kivshar, Y. S. Fano Resonances in Nanoscale Structures. *Rev. Mod. Phys.* **2010**, *82*, 2257−2298.
(13) Luk'yanchuk, B.; Zheludev, N. I.; Maier, S. A.; Halas, N. J.; Nordlander, P.; Giessen, H.; Chong, C. T. The Fano Resonance in Plasmonic Nanostructures and Metamaterials. *Nat. Mater.* **2010**, *9*, 707−715.
(14) Fano, U. Effects of Configuration Interaction on Intensities and Phase Shifts. *Phys. Rev.* **1961**, *124*, 1866−1878.
(15) Hao, F.; Nordlander, P.; Sonnefraud, Y.; Dorpe, P. V.; Maier, S. A. Tunability of Subradiant Dipolar and Fano-Type Plasmon Resonances in Metallic Ring/Disk Cavities: Implications for Nanoscale Optical Sensing. *ACS Nano* **2009**, *3*, 643−652.
(16) Singh, R.; Al-Naib, I.; Yang, Y.; Roy Chowdhury, D.; Cao, W.; Rockstuhl, C.; Ozaki, T.; Morandotti, R.; Zhang, W. Observing Metamaterial Induced Transparency in Individual Fano Resonators with Broken Symmetry. *Appl. Phys. Lett.* **2011**, *99*, 201107−201107.
(17) Zhang, S.; Genov, D. A.; Wang, Y.; Liu, M.; Zhang, X. Plasmon-Induced Transparency in Metamaterials. *Phys. Rev. Lett.* **2008**, *101*, 47401.
(18) Bao, K.; Mirin, N. A.; Nordlander, P. Fano Resonances in Planar Silver Nanosphere Clusters. *Appl. Phys. A: Mater. Sci. Process.* **2010**, *100*, 333−339.
(19) Brown, L. V.; Sobhani, H.; Lassiter, J. B.; Nordlander, P.; Halas, N. J. Heterodimers: Plasmonic Properties of Mismatched Nanoparticle Pairs. *ACS Nano* **2010**, *4*, 819−832.
(20) Bozhevolnyi, S. I.; Evlyukhin, A. B.; Pors, A.; Nielsen, M. G.; Willatzen, M.; Albrektsen, O. Optical Transparency by Detuned Electrical Dipoles. *New J. Phys.* **2011**, *13*, 023034.
(21) Rahmani, M.; Lei, D. Y.; Giannini, V.; Lukiyanchuk, B.; Ranjbar, M.; Liew, T. Y. F.; Hong, M.; Maier, S. A. Subgroup Decomposition of Plasmonic Resonances in Hybrid Oligomers: Modeling the Resonance Lineshape. *Nano Lett.* **2012**, *12*, 2101−2106.
(22) Merchiers, O.; Moreno, F.; González, F.; Saiz, J. Light Scattering by an Ensemble of Interacting Dipolar Particles with Both Electric and Magnetic Polarizabilities. *Phys. Rev. A* **2007**, *76*, 043834.
(23) Doyle, W. T. Optical Properties of a Suspension of Metal Spheres. *Phys. Rev. B* **1989**, *39*, 9852−9858.
(24) Johnson, P. B.; Christy, R. Optical Constants of the Noble Metals. *Phys. Rev. B* **1972**, *6*, 4370−4379.
(25) Xu, Y. L. Radiative Scattering Properties of an Ensemble of Variously Shaped Small Particles. *Phys. Rev. E* **2003**, *67*, 046620.
(26) Wang, M.; Cao, M.; Chen, X.; Gu, N. Subradiant Plasmon Modes in Multilayer Metal−Dielectric Nanoshells. *J. Phys. Chem. C* **2011**, *115*, 20920−20925.